



HAL
open science

Convertible Aircraft Dynamic Modelling and Flatness Analysis

Tudor-Bogdan Airimitoiaie, Gemma Prieto Aguilar, Loïc Lavigne, Christophe Farges, Franck Cazaurang

► **To cite this version:**

Tudor-Bogdan Airimitoiaie, Gemma Prieto Aguilar, Loïc Lavigne, Christophe Farges, Franck Cazaurang. Convertible Aircraft Dynamic Modelling and Flatness Analysis. 9th Vienna International Conference on Mathematical Modelling, Feb 2018, Vienna, Austria. 10.1016/j.ifacol.2018.03.005 . hal-01719054

HAL Id: hal-01719054

<https://hal.science/hal-01719054>

Submitted on 14 Jun 2019

HAL is a multi-disciplinary open access archive for the deposit and dissemination of scientific research documents, whether they are published or not. The documents may come from teaching and research institutions in France or abroad, or from public or private research centers.

L'archive ouverte pluridisciplinaire **HAL**, est destinée au dépôt et à la diffusion de documents scientifiques de niveau recherche, publiés ou non, émanant des établissements d'enseignement et de recherche français ou étrangers, des laboratoires publics ou privés.

Convertible aircraft dynamic modelling and flatness analysis ^{*}

Tudor-Bogdan Airimitoie^{*} Gemma Prieto Aguilar^{*}
Loic Lavigne^{*} Christophe Farges^{*} Franck Cazaurang^{*}

^{*} Univ. Bordeaux, Bordeaux INP, CNRS, IMS, UMR 5218, 33405
Talence, France (e-mail: firstname.lastname@u-bordeaux.fr).

Abstract: This paper describes the dynamic modelling of a vertical take-off and landing (VTOL) aircraft and shows the flatness of the proposed model. Flat systems have the property that the inputs and the states can be written as functions of a set of the system outputs (called flat outputs) and the derivatives of these flat outputs. The flatness property allows to compute an inverse dynamic model of the given system. This can be used in path planning, nonlinear control and fault detection and isolation. The convertible aircraft presented in this paper uses redundant actuators. The advantage of this design is twofold. Firstly, it is possible to configure actuators to optimize both stationary and fast horizontal flight. Secondly, in case of one actuator failure, it provides sufficient flexibility to reconfigure the actuators in order to land safely. An important contribution of this paper is the demonstration of the flatness property for the proposed dynamical model of the convertible aircraft.

Keywords: inverse dynamic problem, flatness, nonlinear models, autonomous vehicles, convertible aircraft

1. INTRODUCTION

In recent years, there has been an increased interest in the topic of unmanned aerial systems (UAS) with the emergence of a new topic which is the modelling and control of convertible aircraft (see Cetinsoy et al. (2012); Yildiz et al. (2015); Wang and Cai (2015); Phung (2015)). One can distinguish two main classes of UAS: multicopters and aircraft. While multicopters have the ability to take-off and land vertically, aircraft can fly over longer distances being able to reach higher speed and longer flight durations. Convertible aircraft try to combine the benefits of both worlds. They are equipped with multiple propeller-engines for vertical take-off and landing but also with aerodynamic lifting surfaces (wings) to increase autonomy and flight distance.

The present paper is the starting point of project MICA (Model Identification and control of a Convertible Aircraft) whose aim is the design of a convertible aircraft embedding robust fault tolerant control algorithms (see MICA (2016)). There are two main technical solutions to achieve conversion from the multicopter configuration (for take-off, landing, or hover) to the aircraft configuration (for horizontal fast forward flight): tilt-rotor and tilt-wing. The main difference is that in the tilt-wing configuration, the propeller-engine and the wing turn together to achieve transition. A tilt-wing solution with six propeller-engines has been chosen for project MICA due to the fact that it allows to control wing angle of attack already from the transition phase to achieve lift as early as possible and reduce consumed energy. This idea is illustrated in Fig. 1.

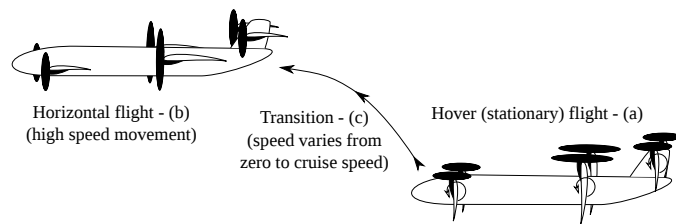


Fig. 1. Hover (a), horizontal flight (b), and transition (c) for a tilt-wing convertible aircraft.

A way to tackle the fault detection and isolation (FDI) problem relies on the flatness theory, which has been introduced for nonlinear systems in Fliess et al. (1992). Since this initial work, the study of flat systems has been further developed. A recent book summarizes most of the results obtained in this domain (see Lévine (2009)). Flatness is a property of some nonlinear systems that can be used to obtain an inverse dynamical model of that system. Some of the applications of this theory can be found in guidance (Morio et al. (2009)), nonlinear controller design (Lavigne et al. (2001)) and FDI (Martínez Torres et al. (2013)).

In this paper, the model of the proposed convertible aircraft is described and it is shown that this model is flat. Based on these results, future work will investigate the design of robust fault tolerant control algorithms. The final objective is to be able to safely land the convertible aircraft in case of failure of one actuator. To achieve this, it is necessary to have a certain degree of actuator redundancy. In case of actuator failure, a fault detection and isolation algorithm should reconfigure the control law to switch from the fault-free-flight actuator set to one of the faulty-flight actuator sets.

^{*} This paper has been supported by the French Agence Nationale de la Recherche (ANR), MICA project.

This paper is organized as follows. Section 2 introduces the notations and conventions that will be used. The convertible aircraft is described in section 3. The nonlinear model is developed using the Newton-Euler formalism in section 5, while the forces and moments which act on the the convertible are given in Section 4. The model uses Euler angles for attitude description. To deal with the gimbal lock problem, a modification to the previous model is proposed in Section 6. The flatness of the full non-linear model is analysed in Section 7. Concluding remarks are given in Section 8.

2. NOTATIONS AND ASSUMPTIONS

Throughout this paper, reference frames are notated with upper-case calligraphic letters. Lower-case italic superscripts indicate projection frames. For example, the inertial frame is denoted as \mathcal{I} and to indicate that a vector has been projected into the inertial frame the superscript i is added to the vector notation.

Let x , y , and z denote the axes of a right-handed coordinate system with origin O . The trigonometric functions \cos , \sin , and \tan will be abbreviated using upright letters c , s , and t , respectively, in the rest of this paper to save space.

Remark: when superscripts are added to the axes notations, they indicate the reference frame to which the axes correspond.

We assume that the gravity field is constant, which implies that the aircraft's center-of-mass (COM) is the same as its center of gravity (CG). We make also the hypothesis of flat and fixed Earth. As such, the origin of the inertial frame (\mathcal{I}) is at the surface of the Earth (usually the position of a ground pilot in the case of UAS). A north-east-down (NED) convention defines the directions of its axes (x^i , y^i , and z^i point respectively towards the North, the East and the center of the Earth).

The vehicle-carried normal Earth (\mathcal{O}) frame, as its name suggests, has its origin located at the CG of the aircraft. Its axes are parallel to those of frame \mathcal{I} . The gravitational force can be written (in frame \mathcal{O}): $G^o = [0 \ 0 \ mg]^T$.

The body frame (\mathcal{B}) has its origin also at the aircraft's CG and its axis x^b , y^b , and z^b point out respectively the nose, the right, and the belly of the aircraft. x^b and z^b define the symmetry plane of the aircraft. Frame \mathcal{B} is related to frame \mathcal{O} through 3 successive rotations: $\phi(t)$, $\theta(t)$, and $\psi(t)$, called the Euler angles. The rotation matrix¹

$$R_b^o = R_z(\psi(t))R_y(\theta(t))R_x(\phi(t)) \quad (1)$$

$$= \begin{bmatrix} c\psi c\phi & -s\psi c\phi + c\psi s\theta s\phi & s\psi s\phi + c\psi s\theta c\phi \\ s\psi c\phi & c\psi c\phi + s\psi s\theta s\phi & -c\psi s\phi + s\psi s\theta c\phi \\ -s\theta & c\theta s\phi & c\theta c\phi \end{bmatrix} \quad (2)$$

can be used to transform a vector from frame \mathcal{B} (subscript b) to frame \mathcal{O} (superscript o), where

$$R_x(\phi) = \begin{bmatrix} 1 & 0 & 0 \\ 0 & c\phi & -s\phi \\ 0 & s\phi & c\phi \end{bmatrix}, \quad R_y(\theta) = \begin{bmatrix} c\theta & 0 & s\theta \\ 0 & 1 & 0 \\ -s\theta & 0 & c\theta \end{bmatrix},$$

¹ In some of the following equations, the parenthesis (t) is dropped to save space.

$$R_z(\psi) = \begin{bmatrix} c\psi & -s\psi & 0 \\ s\psi & c\psi & 0 \\ 0 & 0 & 1 \end{bmatrix}.$$

are the elementary direct rotation matrices (see also Boiffier (1998)). The rotation speed of frame \mathcal{B} with respect to frame \mathcal{O} is denoted Ω_{bo} .

One defines also the kinematic (\mathcal{K}) and aerodynamic (\mathcal{A}) frames whose origins are at the aircraft's CG as well. Frame \mathcal{K} is defined as having the x^k axis pointing in the same direction as the aircraft's kinematic speed ($V_k^k(t) = [v_k(t) \ 0 \ 0]^T$). Frame \mathcal{A} is defined as having the x^a axis pointing in the same direction as the aircraft's aerodynamic speed ($V_a^a(t) = [v_a(t) \ 0 \ 0]^T$). The relation between kinematic, aerodynamic and wind ($V_w(t)$) speeds is given by: $V_k(t) = V_a(t) + V_w(t)$. In this paper, one makes the assumption of negligible wind conditions ($V_w = 0$), which implies that \mathcal{K} and \mathcal{A} are identical ($V_a = V_k$). Frame \mathcal{A} is used in the rest of this paper.

Frames \mathcal{A} (or \mathcal{K}) and \mathcal{B} are related through

$$R_a^b = R_y(-\alpha(t))R_z(\beta(t)) = \begin{bmatrix} c\alpha c\beta & -c\alpha s\beta & -s\alpha \\ s\beta & c\beta & 0 \\ s\alpha c\beta & -s\alpha s\beta & c\alpha \end{bmatrix}, \quad (3)$$

where $\alpha(t)$ is called angle of attack and $\beta(t)$ is the side slip angle. For $v_a(t) = 0$ m/s, frame \mathcal{A} is defined as having the axes aligned with those of frame \mathcal{B} . Frames \mathcal{A} (or \mathcal{K}) and \mathcal{O} are related through 3 successive rotations

$$R_a^o = R_z(\chi(t))R_y(\gamma(t))R_x(\mu(t)) \quad (4)$$

$$= \begin{bmatrix} c\chi c\gamma & -s\chi c\mu + c\chi s\gamma s\mu & s\chi s\mu + c\chi s\gamma c\mu \\ s\chi c\gamma & c\chi c\mu + s\chi s\gamma s\mu & -c\chi s\mu + s\chi s\gamma c\mu \\ -s\gamma & c\gamma s\mu & c\gamma c\mu \end{bmatrix}. \quad (5)$$

An important property of rotation matrices is that they are orthogonal, i.e. they are invertible and the inverse is equal to the transpose ($R_z^y = (R_z^y)^{-1} = (R_z^y)^T$).

The skew-symmetric operator $[\cdot]_{\times}$, of a vector $W = [w_1 \ w_2 \ w_3]^T \in \mathbb{R}^3$, is defined as (Zhao (2016))

$$[W]_{\times} = \begin{bmatrix} 0 & -w_3 & w_2 \\ w_3 & 0 & -w_1 \\ -w_2 & w_1 & 0 \end{bmatrix}. \quad (6)$$

This operation is useful for time derivative calculus of a rotation matrix.

Lifting surfaces on an aircraft produce aerodynamic forces and moments. Let denote the total aircraft aerodynamic force coefficients in frame \mathcal{A} as C_x (drag), C_y (lateral force), and C_z (lift) and in frame \mathcal{B} as C_A (axial force), C_Y (side force), and C_N (normal force). These coefficients are related through the rotation matrix between the body and the aerodynamic frames as

$$[-C_x \ C_y \ -C_z]^T = R_b^a \cdot [-C_A \ C_Y \ -C_N]^T. \quad (7)$$

The aerodynamic moments coefficients are given in frame \mathcal{B} by C_l (rolling moment), C_m (pitching moment), and C_n (yawing moment).

The mass of the aircraft is denoted by m and the gravitational acceleration by g . The inertia matrix in frame \mathcal{B} considering the symmetry of the aircraft can be written

$$I = \begin{bmatrix} I_{xx} & 0 & -I_{xz} \\ 0 & I_{yy} & 0 \\ -I_{xz} & 0 & I_{zz} \end{bmatrix}. \quad (8)$$

3. SYSTEM DESCRIPTION

Figures 2 and 3 show the convertible aircraft concept proposed in this paper. A view from the left side is given in Fig. 2 and a second from above is presented in Fig. 3. The orientation of the body frame \mathcal{B} axes can be observed: x^b points to the front of the aircraft and belongs to its plane of symmetry alongside z^b axis, which is perpendicular to x^b and pointing towards the Earth. The y^b axis is perpendicular to the symmetrical plane and oriented towards the right of the aircraft.

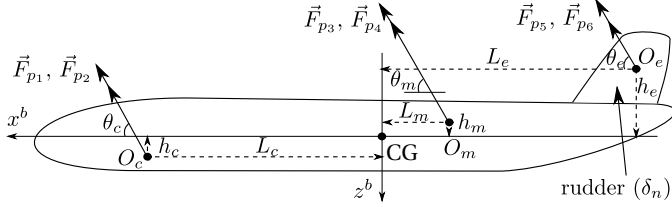


Fig. 2. MICA convertible aircraft - view from left side.

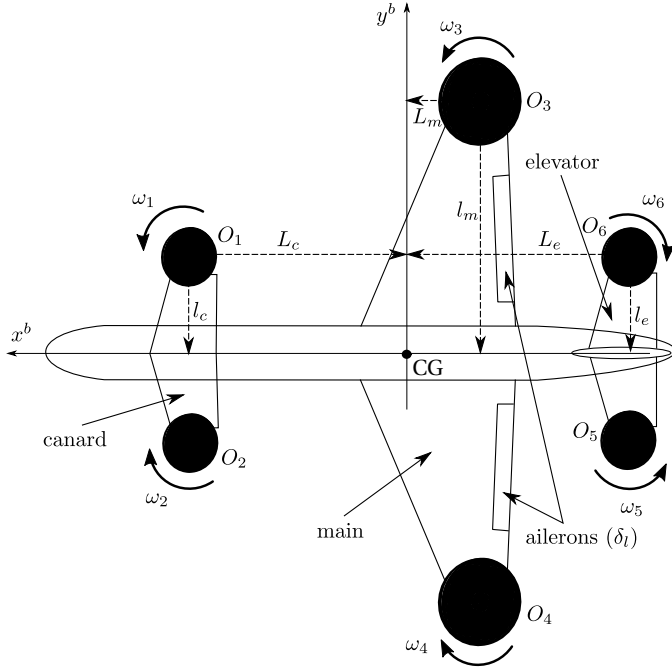


Fig. 3. MICA convertible aircraft - view from above.

As it can be seen in Fig. 3, the convertible aircraft has 3 pairs of wings: canard (in front), main (in the middle) and elevator (in the back). Each pair can turn around an axis perpendicular to the aircraft's symmetry plane. \mathcal{W}_j is the reference frame related to wing j ($\forall j \in \{c$ (canard), m (main), e (elevator) $\}$). The rotation matrix between frames \mathcal{W}_j and \mathcal{B} is given as

$$R_j^b = R_y(\theta_j(t)) = \begin{bmatrix} c\theta_j & 0 & s\theta_j \\ 0 & 1 & 0 \\ -s\theta_j & 0 & c\theta_j \end{bmatrix}, \quad \forall j \in \{c, m, e\}, \quad (9)$$

where θ_j is the tilt angle between the chord of wing j and the x^b axis. For $\theta_j = 0$, the axes of \mathcal{W}_j are parallel to those of the body frame. The origin of the \mathcal{W}_j is denoted as O_j , $\forall j \in \{c, m, e\}$ and it is located on the intersection between the aircraft's symmetry plane and the rotation

axis. The origin points and the angles of rotation are indicated in Fig. 2.

There are 2 propeller-engines on each wing, situated symmetrically at the extreme wing positions. The engines are fixed on the wings. For each engine, the distance to the CG is indicated in Figs. 2 and 3 as L_i (on x^b axis), l_i (on y^b axis), and h_i (on z^b axis), $\forall i \in \{c, m, e\}$.

There are 11 control inputs on this convertible aircraft concept: the 3 wing rotation angles (θ_c , θ_m , and θ_e), the rotation speeds of 6 propeller-engines (ω_1 , ω_2 , ω_3 , ω_4 , ω_5 , and ω_6), the main wing aileron deflection (δ_l), and the rudder tilt angle (δ_n).

As in conventional aircraft, the main wing ailerons receive the same control input but they have opposite senses of rotation. With the exception of the main wing, the other aerodynamic surfaces (canard, elevator, and rudder) have symmetrical profiles. The propeller-engines 1, 2, 5, and 6 are supposed identical. Also propeller-engine 3 is supposed identical to 4. The senses of rotation of each propeller are indicated in Fig. 3.

Some of the 11 inputs available on the convertible aircraft are redundant. This redundancy is necessary in the design of fault tolerant control algorithms for autonomous flight. In fault-free conditions, only 5 control inputs are used depending on the flight phase.

Take-off, landing, and hover: During this phase of the flight (essentially when $V_a^a(t)$ is small), only ω_1 , ω_2 , ω_5 , ω_6 , and $\theta_c = \theta_e$ (canard and elevator wings are tilted with the same angle) are used. Concerning the unused actuators: $\omega_3 = \omega_4 = 0$ rad/s, $\theta_m = 90^\circ$ (main wing chord perpendicular to the x^b axis), $\delta_l = 0$, and $\delta_n = 0$.

Fast forward flight: During this phase of the flight, only ω_3 , ω_4 , δ_l , δ_n , and θ_c are used. Concerning the unused actuators: $\omega_1 = \omega_2 = \omega_5 = \omega_6 = 0$, θ_m is fixed at a positive angle close to 0 (the exact value should be chosen taking into account aerodynamic characteristics, desired autonomy and performance). θ_e is modified during fast forward flight so that the angle of attack of the elevator is zero and no force or moment is produced by it.

Due to its effect on the pitch of the aircraft, θ_c is also denoted δ_m .

4. FORCES AND MOMENTS

4.1 Propulsion forces and moments

Let consider the index notation

$$(j, h) \in \{(c, \{1, 2\}), (m, \{3, 4\}), (e, \{5, 6\})\}, \quad (10)$$

which signifies that for a given $j \in \{c, m, e\}$, h can have either one of two values. Each propeller-engine generates a propulsion force and a couple of drag. Expressed in their corresponding wing reference frame, these are given, respectively, by

$$F_{p_h}^j(t) = [k_j \omega_h^2 \ 0 \ 0]^T, \quad \tau_h^j(t) = [(-1)^h d_j \omega_h^2 \ 0 \ 0]^T, \quad (11)$$

where k_j and d_j are constants which depend on the physical characteristics of the propellers.

Remark: the propellers on the canard and elevator wings are supposed to be identical, optimized for hover flight

(such that $k_c = k_e$), while the propellers on the main wing are optimized for horizontal flight.

The propulsion force of one set of propeller-engines (located on the same wing) is given by

$$F_{p_j}^j(t) = \sum_h F_{p_h}^j(t) \quad (12)$$

Using (12), the propulsion force due to all 6 helices (in the body frame \mathcal{B}) is given by

$$F_p^b(t) = \begin{bmatrix} X_p^b(t) \\ 0 \\ Z_p^b(t) \end{bmatrix} = \sum_{j=\{c,m,e\}} R_y(\theta_j) F_{p_j}^j(t). \quad (13)$$

Each propulsion force induces also a moment which can be written as

$$M_{p_h}(t) = \overrightarrow{(CG, O_h)} \wedge F_{p_h}(t). \quad (14)$$

The points O_h (see Fig. 3) represent the application points of each propulsion force. These moments can be projected in the body frame as

$$M_{p_h}^b(t) = \overrightarrow{(CG, O_h)}|_{\mathcal{B}} \wedge F_{p_h}^b(t), \quad (15)$$

where $F_{p_h}^b(t) = R_j^b F_{p_h}^j(t)$, $\forall (j, h)$ given by (10). The sum of the 6 propulsion moments is $M_p^b(t) = \sum_{h=1}^6 M_{p_h}^b(t)$.

The sum of the drag couples can be written, in \mathcal{B} , as

$$\tau_d^b(t) = R_c^b(\tau_1^c + \tau_2^c) + R_m^b(\tau_3^m + \tau_4^m) + R_e^b(\theta_e)(\tau_5^e + \tau_6^e). \quad (16)$$

4.2 Aerodynamic forces and moments

As noted in Section 2, the aerodynamic force coefficients C_x , C_y , and C_z represent the combined effect of all aerodynamic surfaces on the force vector in the aerodynamic frame. As such, the aerodynamic force vector can be written (in frame \mathcal{A}) as

$$F_a^a(t) = \begin{bmatrix} X_a^a(t) \\ Y_a^a(t) \\ Z_a^a(t) \end{bmatrix} = \frac{1}{2} \rho S V_a^a(t)^2 \begin{bmatrix} -C_x(t) \\ C_y(t) \\ -C_z(t) \end{bmatrix} \quad (17)$$

Similarly, C_l , C_m , and C_n represent the combined aerodynamic effects on the torques of the aircraft. The torques vector can be given in frame \mathcal{B} as

$$\tau_a^b(t) = \begin{bmatrix} L_a^b(t) \\ M_a^b(t) \\ N_a^b(t) \end{bmatrix} = \frac{1}{2} \rho S l V_a^a(t)^2 \begin{bmatrix} C_l(t) \\ C_m(t) \\ C_n(t) \end{bmatrix}. \quad (18)$$

C_x , C_y , C_z , C_l , C_m , and C_n are nonlinear functions depending in general on the profile of the various aerodynamic surfaces, the Reynolds number Re (which depends also on V_a^a), the tilt angles (θ_c , θ_m , θ_e), the aileron deflection (δ_l), the rudder tilt angles (δ_n), the translational speed (V_a^a , α , β), acceleration (\dot{V}_a^a , $\dot{\alpha}$, $\dot{\beta}$), and the rotational speed (p , q , r). In practice, simplified mathematical expressions for these coefficients can be found using wind tunnel and flight data (for example, in Martin (1992) the expressions of these coefficients for an F4 fighter jet are given).

4.3 Total forces and moments

Let denote the total force vector from propulsion and aerodynamic elements, in frame \mathcal{A} , as

$$F^a = \begin{bmatrix} X^a(t) \\ Y^a(t) \\ Z^a(t) \end{bmatrix} = F_a^a(t) + (R_a^b)^T F_p^b(t) \quad (19)$$

The total torque vector is given, in frame \mathcal{B} , by

$$\tau^b = \begin{bmatrix} L^b(t) \\ M^b(t) \\ N^b(t) \end{bmatrix} = \tau_a^b + M_p^b(t) + \tau_d^b(t) \quad (20)$$

5. NONLINEAR MODEL OF THE CONVERTIBLE AIRCRAFT

This section describes the development of the nonlinear model for the convertible aircraft using the Newton-Euler formalism. There exist various choices of frames for writing the equations for the translational and rotational motion. In this paper, we have decided to write the equations for the translational motion in frame \mathcal{A} and those for the rotational motion in frame \mathcal{B} (more details can be found in Martin (1992); Boiffier (1998)):

$$\dot{\xi} = R_a^o V_a^a, \quad (21)$$

$$m \frac{dV_a^a}{dt} + \Omega_{ao}^a \wedge m V_a^a = F^a + (R_a^o)^T G^o, \quad (22)$$

$$\dot{R}_a^o = R_a^o [\Omega_{ao}^a]_{\times}, \quad (23)$$

$$\frac{d(I\Omega_{bo}^b)}{dt} + \Omega_{bo}^b \wedge I\Omega_{bo}^b = \tau_b, \quad (24)$$

where $\xi = [x \ y \ z]^T$ gives the position of the center of mass of the aircraft relative to frame \mathcal{I} . The elements of Ω_{bo}^b are denoted $\Omega_{bo}^b = [p \ q \ r]^T$. The skew-symmetric operator $[\cdot]_{\times}$ has been defined in Section 2.

It is necessary to find a relation between Ω_{ao}^a and Ω_{bo}^b . The following property is known: $\Omega_{ao}^a = \Omega_{ab}^a + \Omega_{bo}^b$. Projecting this equation in frame \mathcal{A} gives

$$\Omega_{ao}^a = \Omega_{ab}^a + R_b^a \Omega_{bo}^b. \quad (25)$$

Using

$$\dot{R}_a^b = R_a^b [\Omega_{ab}^a]_{\times} \implies [\Omega_{ab}^a]_{\times} = (R_a^b)^T \dot{R}_a^b, \quad (26)$$

it is possible to find the elements of Ω_{ab}^a as functions of angles $\alpha(t)$, $\beta(t)$, and their derivatives

$$\Omega_{ab}^a = [-\dot{\alpha} s \beta \quad -\dot{\alpha} c \beta \quad \dot{\beta}]^T \quad (27)$$

Introducing (27) in (25), the desired expression of Ω_{ao}^a as function of Ω_{bo}^b is obtained. The complete system of equations is detailed in (28).

$$\dot{x}(t) = c \chi c \gamma V_a^a, \quad \dot{y}(t) = s \chi c \gamma V_a^a, \quad \dot{z}(t) = -s \gamma V_a^a, \quad (28.1)$$

$$\dot{V}_a^a(t) = \frac{X^a}{m} - s \gamma g, \quad (28.2)$$

$$\dot{\beta}(t) = s \alpha p - c \alpha r + \frac{c \gamma s \mu m g + Y^a}{m V_a^a}, \quad (28.3)$$

$$\dot{\alpha}(t) = q - (c \alpha p + s \alpha r) t \beta + \frac{c \gamma c \mu}{c \beta} \frac{g}{V_a^a} + \frac{Z^a}{c \beta m V_a^a}, \quad (28.4)$$

$$\dot{\chi}(t) = \frac{-Z^a s \mu + Y^a c \mu}{V_a^a m c \gamma}, \quad (28.5)$$

$$\dot{\gamma}(t) = \frac{-c \gamma g m - Y^a s \mu - Z^a c \mu}{V_a^a m}, \quad (28.6)$$

$$\dot{\mu}(t) = \frac{-c \mu c \gamma s \beta g}{V_a^a c \beta} + \frac{p c \alpha + r s \alpha}{c \beta} - \frac{Z^a s \beta}{V_a^a m c \beta}$$

$$+ \frac{s\gamma(Y^a c\mu - Z^a s\mu)}{V_a^a m c\gamma}, \quad (28.7)$$

$$\dot{p}(t) = \frac{(I_{xz}(I_{xx} - I_{yy} + I_{zz})p - (I_{xz}^2 - I_{zz}(I_{yy} - I_{zz}))r)q}{I_{xx}I_{zz} - I_{xz}^2} + \frac{I_{xz}N^b + I_{zz}L^b}{I_{xx}I_{zz} - I_{xz}^2}, \quad (28.8)$$

$$\dot{q}(t) = \frac{-I_{xz}p^2 - r(I_{xx} - I_{zz})p + I_{xz}r^2 + M^b}{I_{yy}}, \quad (28.9)$$

$$\dot{r}(t) = \frac{((I_{xz}^2 + I_{xx}(I_{xx} - I_{yy}))p - I_{xz}(I_{xx} - I_{yy} + I_{zz})r)q}{I_{xx}I_{zz} - I_{xz}^2} + \frac{I_{xx}N^b + I_{xz}L^b}{I_{xx}I_{zz} - I_{xz}^2}. \quad (28.10)$$

Remarks: (i) use of R_a^o matrix in (21) simplifies the equations and eases the study of the flatness of the model as will be later shown. (ii) Ω_{bo}^b is preferred due to the practical reasons concerning the estimation of p , q , and r .

6. GIMBAL LOCK AND VERTICAL EULER ANGLES

The use of the Euler angles $\mu(t)$, $\gamma(t)$, and $\chi(t)$ for the R_a^o introduces a gimbal lock problem for $\gamma(t)$ close to 90° . This can be an issue for the proposed convertible aircraft during take-off and landing, when the speed vector is oriented vertically.

To deal with this issue, a modified model using vertical Euler angles $\mu_v(t)$, $\gamma_v(t)$, and $\chi_v(t)$ is proposed in this section. The rotation between frames using vertical Euler angles has been presented previously in Castillo et al. (2005). To assure that an angle $\gamma_v(t)$ smaller than 90° is obtained when the convertible aircraft is flying vertically, the rotation matrix in (29) is used.

$$R_{a_v}^o = R_y(\pi/2)R_z(\chi_v(t))R_y(\gamma_v(t))R_x(\mu_v(t)) \quad (29)$$

Equations (28.1)–(28.7) are modified as shown in (30.1)–(30.8). Equations (28.8)–(28.10) remain the same.

$$\dot{x}(t) = -s\gamma_v V_a^a, \quad \dot{y}(t) = s\chi_v c\gamma_v V_a^a, \quad (30.1)$$

$$\dot{z}(t) = -c\chi_v c\gamma_v V_a^a, \quad (30.2)$$

$$\dot{V}_a^a(t) = \frac{X^a}{m} - c\chi_v c\gamma_v g, \quad (30.3)$$

$$\dot{\beta}_v(t) = \frac{-s\gamma_v s\mu_v c\chi_v g}{V_a^a} + \frac{s\chi_v c\mu_v g}{V_a^a} + p s\alpha_v - r c\alpha_v + \frac{Y^a}{m V_a^a}, \quad (30.4)$$

$$\dot{\alpha}_v(t) = q - c\alpha_v p + s\alpha_v r t \beta_v - \frac{c\mu_v s\gamma_v c\chi_v g}{V_a^a c\beta_v} - \frac{s\chi_v s\mu_v g}{V_a^a c\beta_v} + \frac{Z^a}{V_a^a m c\beta_v}, \quad (30.5)$$

$$\dot{\chi}_v(t) = \frac{s\chi_v g m - Z^a s\mu_v + Y^a c\mu_v}{c\gamma_v V_a^a m}, \quad (30.6)$$

$$\dot{\gamma}_v(t) = \frac{c\chi_v s\gamma_v g m - Z^a c\mu_v - Y^a s\mu_v}{V_a^a m}, \quad (30.7)$$

$$\dot{\mu}_v(t) = \frac{(c\chi_v c\mu_v s\gamma_v + s\chi_v s\mu_v) g s\beta_v}{V_a^a c\beta_v} + \frac{c\alpha_v p + s\alpha_v r}{c\beta_v} + \frac{s\gamma_v (s\chi_v g m - Z^a s\mu_v + Y^a c\mu_v)}{c\gamma_v V_a^a m} - \frac{Z^a s\beta_v}{V_a^a c\beta_v m}. \quad (30.8)$$

Remark: the explicit systems of equations (28) and (30) become implicit at hover ($v_a(t) = 0$ m/s).

7. FLATNESS OF THE OBTAINED MODEL

In this section, the flatness of the obtained convertible aircraft model is addressed. Let begin by briefly recalling the concept of a flat system (more detailed presentations can be found in Martin (1992); Fliess et al. (1995); Morio et al. (2009)). Consider the nonlinear system

$$\dot{x} = f(x, u), \quad (31)$$

where $x \in \mathbb{R}^n$ is the state and $u \in \mathbb{R}^m$ is the control vector with $m \leq n$. System (31) is call (differentially) flat if, and only if, there exists a m -dimensional vector $y = y(x, u, \dot{u}, \dots, u^n)$, such that x and u can be expressed as functions of the components of y and a finite number of their time derivatives.

Let consider the model given in (28.1)–(28.10), where the functions describing the aerodynamic forces and moments coefficients are supposed known, as well as the air density ρ and the wing area S .

As mentioned in Section 3, at any time, only a set of 5 independent control inputs are used. As such, 5 independent flat outputs should be found. Assume that $x(t)$, $y(t)$, $z(t)$, $\alpha(t)$, and $\beta(t)$ are the flat outputs of the system. To show that the convertible aircraft model is flat, one has to find functions for the other state variables and control inputs depending only on the proposed flat outputs and their derivatives.

Instead of trying to find directly the control inputs, initially the expressions for the total forces and moments are searched. Nevertheless, an assumption is necessary to reduce the number of unknowns to five. It is assumed that $C_Y(t) = 0$, which corresponds to a side slip angle β equal to zero. Using (19), one obtains

$$\begin{bmatrix} X^a(t) \\ Y^a(t) \\ Z^a(t) \end{bmatrix} = \frac{1}{2} \rho S V_a^a(t)^2 \begin{bmatrix} -C_x(t) \\ C_y(t) \\ -C_z(t) \end{bmatrix} + (R_a^b)^T \begin{bmatrix} X_p^b(t) \\ 0 \\ Z_p^b(t) \end{bmatrix} \\ \implies R_a^b \begin{bmatrix} X^a(t) \\ Y^a(t) \\ Z^a(t) \end{bmatrix} = \frac{1}{2} \rho S V_a^a(t)^2 \begin{bmatrix} -C_A(t) \\ C_Y(t) \\ -C_N(t) \end{bmatrix} + \begin{bmatrix} X_p^b(t) \\ 0 \\ Z_p^b(t) \end{bmatrix}$$

If $C_Y(t) = 0$, from the second line of the previous matrix equation one obtains:

$$[s\beta \ c\beta \ 0] \begin{bmatrix} X^a \\ Y^a \\ Z^a \end{bmatrix} = 0 \implies Y^a(t) = -t\beta(t)X^a(t) \quad (32)$$

Remark: from a controller design perspective, the side slip angle β will be steered towards zero guaranteeing $C_Y(t) = 0$. This can be obtained using robust control (see also Lavigne et al. (2001)).

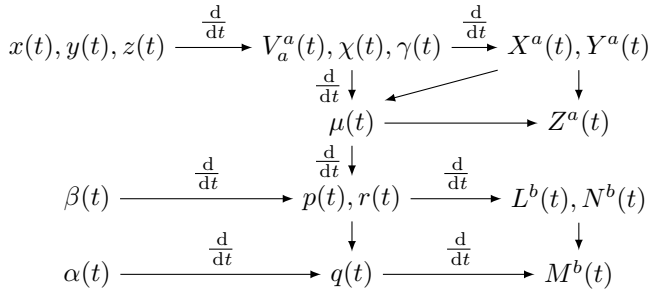
From (28.1), it is straightforward to obtain the equations for $V_a^a(t)$, $\chi(t)$, $\gamma(t)$ as functions of the flat outputs and their first derivatives. Subsequently, the expression of $X^a(t)$ can be obtained by time deriving the expression for $V_a^a(t)$ and using (28.2). Using (32), the expression for $Y^a(t)$ is also obtained.

8. CONCLUSIONS

The expressions for $\mu(t)$ and $Z^a(t)$ are obtained from (28.5) and (28.6). Subsequently, it is possible to deduce $p(t)$ and $r(t)$ from (28.3) and (28.7) and the time derivative of $\beta(t)$. Then $q(t)$ is calculated introducing also (28.4) and the time derivative of $\alpha(t)$.

Equations (28.8)–(28.10) allow to deduce the moments applied to the aircraft. First $L^b(t)$ and $N^b(t)$ are obtained from (28.8) and (28.10), then $M^b(t)$ is calculated from (28.9) after one last time derivation.

The following diagram resumes this discussion. The flat outputs are on the left, the other states are in the middle and the system inputs are on the right column. The successive derivations can be observed:



Depending on the flight mode, X^a , Y^a , Z^a , L^b , M^b and N^b allow to obtain the expressions of the true control inputs.

Take-off, landing, and hover: In this phase of the flight, the contribution of the aerodynamic forces and moments are negligible. As such, the assumption $C_Y(t) = 0$ is valid. Using (19) and the expressions for X^a , Y^a , Z^a , α , and β , one obtains

$$X_p^b(t) = [cac\beta - cas\beta - s\alpha] \cdot [X^a(t) Y^a(t) Z^a(t)]^T \quad (33)$$

$$Z_p^b(t) = [sac\beta - sas\beta c\alpha] \cdot [X^a(t) Y^a(t) Z^a(t)]^T \quad (34)$$

Given that $\omega_3(t) = \omega_4(t) = 0$ and $\theta_c(t) = \theta_e(t)$ (\mathcal{W}_c and \mathcal{W}_e have parallel axes), projecting (13) in frame \mathcal{W}_e , one obtains

$$\begin{bmatrix} X_p^b(t) \\ 0 \\ Z_p^b(t) \end{bmatrix} = R_y(\theta_c) (F_{p_1}^c + F_{p_2}^c + F_{p_5}^c + F_{p_6}^c). \quad (35)$$

From (33) and (34), one can then compute the canard and elevator tilt $\theta_c = \theta_e$ and the propulsion force $(F_{p_1}^c + F_{p_2}^c + F_{p_5}^c + F_{p_6}^c)$.

Fast forward flight: It is assumed that the point O_m in Fig. 2 coincides with the CG (by construction it is possible to obtain very small L_m and h_m). As such, the propulsion force does not generate a moment. Then the expression L^b , M^b , and N^b allow to obtain the equations for δ_l , θ_c , and δ_n , respectively. Subsequently, X_p^b and Z_p^b can be obtained which allow to write the expressions for ω_3 and ω_4 .

Remark: a similar procedure can be used to show that the model in (30.1)–(30.8), (28.8)–(28.10) is flat with the same set of flat outputs under the assumption that $C_Y(t) = 0$.

The nonlinear modelling for a convertible aircraft using redundant actuators has been presented. It has been shown that the proposed model has the property of flatness. This result is the base of future research that will focus on designing fault tolerant robust control algorithms.

REFERENCES

- Boiffier, J.L. (1998). *The dynamics of flight - the equations*. John Wiley & Sons, Chichester.
- Castillo, P., Lozano, R., and Dzul, A.E. (2005). *Modelling and control of mini-flying machines*. Springer Verlag London.
- Cetinsoy, E., Dikyar, S., Hancer, C., Oner, K., Sirimoglu, E., Unel, M., and Aksit, M. (2012). Design and construction of a novel quad tilt-wing uav. *Mechatronics*, 22(6), 723 – 745. Special Issue on Intelligent Mechatronics (LSMS2010 & ICSEE2010).
- Fliess, M., Lévine, J., Martin, P., and Rouchon, P. (1992). Sur les systèmes non linéaires différentiellement plats. *Comptes rendus de l'Académie des sciences. Série 1, Mathématique*, 315(5), 619–624.
- Fliess, M., Lévine, J., Martin, P., and Rouchon, P. (1995). Flatness and defect of non-linear systems: introductory theory and examples. *International Journal of Control*, 61(6), 1327–1361.
- Lavigne, L., Cazaurang, F., and Bergeon, B. (2001). Modeling of disturbed flat system for robust control design. *IFAC Proceedings Volumes*, 34(6), 759 – 762. 5th IFAC Symposium on Nonlinear Control Systems 2001, St Petersburg, Russia, 4-6 July 2001.
- Lévine, J. (2009). *Analysis and Control of Nonlinear Systems. A Flatness-based Approach*. Springer-Verlag Berlin Heidelberg.
- Martin, P. (1992). *On differentially flat systems*. Theses, École Nationale Supérieure des Mines de Paris.
- Martínez Torres, C., Lavigne, L., Cazaurang, F., Alcorta García, E., and Díaz Romero, D. (2013). Fault detection and isolation on a three tank system using differential flatness. In *2013 European Control Conference (ECC)*, 2433–2438.
- MICA (2016). Model Identification and Control of a convertible Aircraft, French National Research Agency (ANR). <http://tudor-bogdan.airimitoiaie.name/mica/>.
- Morio, V., Cazaurang, F., and Vernis, P. (2009). Flatness-based hypersonic reentry guidance of a lifting-body vehicle. *Control Engineering Practice*, 17(5), 588 – 596.
- Phung, D.K. (2015). *Conception, modeling, and control of a convertible mini-drone*. Theses, Université Pierre et Marie Curie - Paris VI.
- Wang, X. and Cai, L. (2015). Mathematical modeling and control of a tilt-rotor aircraft. *Aerospace Science and Technology*, 47, 473 – 492.
- Yildiz, Y., Unel, M., and Demirel, A.E. (2015). Adaptive nonlinear hierarchical control of a quad tilt-wing uav. In *2015 European Control Conference (ECC)*, 3623–3628.
- Zhao, S. (2016). Time derivative of rotation matrices: A tutorial. *CoRR*, abs/1609.06088. URL <http://arxiv.org/abs/1609.06088>.